



# Influence of the glass transition temperature gradient on the non-linear viscoelastic behavior in reinforced elastomers

Helene Montes, Francois Lequeux, Julien Berriot

## ► To cite this version:

Helene Montes, Francois Lequeux, Julien Berriot. Influence of the glass transition temperature gradient on the non-linear viscoelastic behavior in reinforced elastomers. *Macromolecules*, 2003, 36 (21), pp.8107-8118. 10.1021/ma0344590 . hal-02530969

**HAL Id: hal-02530969**

**<https://hal.science/hal-02530969>**

Submitted on 6 Apr 2020

**HAL** is a multi-disciplinary open access archive for the deposit and dissemination of scientific research documents, whether they are published or not. The documents may come from teaching and research institutions in France or abroad, or from public or private research centers.

L'archive ouverte pluridisciplinaire **HAL**, est destinée au dépôt et à la diffusion de documents scientifiques de niveau recherche, publiés ou non, émanant des établissements d'enseignement et de recherche français ou étrangers, des laboratoires publics ou privés.

# Influence of the glass transition temperature gradient on the non-linear viscoelastic behavior in reinforced elastomers.

*H.Montes\*, F. Lequeux and J. Berriot*

ESPCI, 10 Rue Vauquelin, 75005 Paris

\*Corresponding author: [Helene.montes@espci.fr](mailto:Helene.montes@espci.fr)

## **Abstract :**

We analyze the influence of a glass transition gradient near the particle surfaces on the non-linear mechanical behavior of reinforced elastomers. We studied systems consisting in grafted silica particles dispersed in a cross-linked poly(ethylacrylate) matrix. Both particle/matrix interfaces and dispersion states of the particles have been precisely characterized. Based on previous studies on the same systems evidencing a glass transition gradient around the particles, we show that the precocious non-linear mechanical behavior of these filled systems is related to the strain-softening of the glassy polymer shell surrounding the particles surfaces. Comparing strain-softening and melting of the glassy polymer shell, we observe that the strain-softening is enhanced by strong local stress amplifications.

## Introduction

Filled rubber, consisting in solid particles –either carbon black or silica – dispersed in an elastic matrix, have been widely used in current life for more than fifty years. The role of the solid particles is to reinforce the elastic matrix, increasing both elastic modulus, fracture and abrasion properties. However, most of their mechanical properties are far to be understood. This is mostly due to the intricate effects of solid particles arrangements in the elastic matrix and of modifications of the polymer dynamics near the surface of the particles. These two effects have been the objects of various approaches.

First, the arrangement of the particles –generally dispersed as fractal aggregates - contributes in a complex manner to both the linear and the non-linear mechanical properties of filled rubbers, and various approaches have been proposed in the past and more recently [1,2,3,4]. The main idea is that fractal aggregates can strongly increase the elastic modulus. But under strain there is an evolution of their fractal geometry leading to a decrease of the value of the elastic modulus. This so-called hydrodynamic reinforcement effect is however difficult to quantitatively describe, as it requires a very precise knowledge of the particles arrangement.

Secondly, the modification of the polymer dynamics near the surface of the particles has been more puzzling. It has been suggested that dynamics of adsorption/desorption of the polymers chains at the particle surface may be responsible for various linear and non-linear effects [5,6]. Here, we present results on samples where the polymer chains are strongly anchored, through covalent bonds to the surface of the particles. Thus the effects of polymer adsorption-desorption is not relevant in our case. Otherwise, in the past, it has been suggested by Struik and others authors [7-10] that the particle/elastomer interface generates around each particle a shell of glassy polymer. For instance, Struik [7,8] has quenched filled rubber above its glass transition temperature and he observed a physical aging behaviour similar to the one shown by a glassy polymer below its glass transition temperature ( $T_g$ ). NMR measurements have confirmed the glassy nature of the polymer chains near the particles surface

[9-10]. This idea was recently improved in introducing the concept that there is a gradient of glass transition temperature around each particle. This was first suggested by [11] and quantified by us, on model filled elastomers, both using N.M.R. and mechanical data [12, 13]. This idea is also confirmed by the various experiments of  $T_g$  measurements performed on polymer films casted on various substrates [14-17]. Lastly this is consistent with recent simulations [18,19] and some theoretical explanations were proposed recently [20]. Actually, we will show in this paper that this concept can also help to understand mechanical non-linearities in filled elastomers.

In fact, as explained in [3], the combination of the two effects – surface dynamics of polymers and particles arrangement in the sample – is required to explain the mechanical properties of filled rubber. But the building of a theoretical frame combining these two effects is difficult and is still a challenge for the community.

In this paper we will focus on the role of the polymer dynamics near the particle surface on the non-linearity shown by the dynamical elastic modulus for small values of strain – typically below 100%. This non-linearity is in fact a decrease of the dynamical elastic modulus for increasing the strain amplitude and has been known for years as the Payne effect in the reinforced elastomer community [21]. In this paper we will show how the gradient of glass transition is responsible for the Payne effect in filled rubbers.

The paper is organized as follows. First we recall the samples preparation procedures, and present the mechanical measurements. Then we recall how we have evidenced the gradient of glass transition on filled elastomers, using linear mechanical properties. Then we discuss the Payne effect in the frame of this concept. According to bulk polymers behaviour, we assume that the glassy polymer chains near the particles soften under strain. We then validate this assumption using an original time-temperature superposition for the non-linear dynamical elastic modulus. Finally, we discuss the possibility of comparing temperature versus stress effects for the non-linearities of the dynamical modulus. We suggest lastly a hand-waving description of the stress heterogeneities that provides a qualitatively description of the observed effects.

## Experimental section

### A) Samples preparation

The mechanical measurements were performed on cross-linked polyethylacrylate chains reinforced with grafted silica particles. The process used for their synthesis have been presented in details in a previous paper [22]. We briefly recall here the main steps of the preparation.

**Table I : Characteristics of the reinforced sample sets and the non reinforced elastomer matrix.**

| Set name    | Mean Silica diameter<br>(nm) <sup>1</sup> | Grafting Density<br>$\Gamma$<br>(nm <sup>-2</sup> ) | e <sub>Graft</sub><br>(nm) | Crosslinker Concentration<br><sub>2</sub><br>(%) | $\langle f_{si}^N \rangle$<br>(nm <sup>-2</sup> ) <sup>3</sup> | $v_{tot}/v_e$ <sup>3</sup> | $\delta$<br>(nm) <sup>3</sup> |
|-------------|---|---|----------------------------|--|--|----------------------------|-------------------------------|
| EA          | -   | -   | -                          | 0.3  | -  | 1.58                       | -                             |
| MCS_I/C*    | 45 ± 5                                    | 1.6 ± 0.5   | 0.52                       | 0.3  | 2.25   | [1.84, 3] <sup>4</sup>     | 0.12                          |
| ACS/C**     | 54 ± 7                                    | 2. ± 0.5  | 0.3                        | 0.3  | 0  | 1.58                       | < 0.1                         |
| MCS_II/H*** | 50 ± 7                                    | 2.8 ± 0.5   | 0.6                        | 0.3  | 1.0  | [1.67, 1.9] <sup>4</sup>   | 0.25                          |
| TPM_III/C*  | 80 ± 7                                    | 10.5 ± 1  | 1.3                        | 0.3  | 1.7  | [1.7, 2] <sup>4</sup>      | 0.5                           |
| TPM_VI/C*   | 50 ± 7                                    | 1.5 ± 0.5   | 0.3                        | 0.3  | 1.1  | [1.6, 2]                   | 0.2                           |

1 : from SANS measurements [21].Dispersion state from SANS measurements,\*: there is an exclusion radius around the particles, \*\*: presence of large aggregates; \*\*\* : there is the coexistence of any linear aggregates with single particles. 2: per mole of ethylacrylate monomers. 3: from <sup>1</sup>H NMR measurements [23], 4: depending on the silica volume fraction.

Following the process developed by Ford and Mauger [23, 24], spherical silica particles are prepared using the Stöber method. They are either transferred to propyl carbonate before to be grafted by monochloro silane molecules -3 methacryloxy propyl dimethylchlorosilane (MCS) or acetoxylethyl-

dimethylchlorosilane (ACS) - or directly grafted in the stöber solution with 3 - trimethoxysilylpropylmethacrylate (TPM). The grafted silica are then transferred by successive dialysis to methanol and then to ethylacrylate monomers. From a concentrated parent suspension of silica particle in acrylate monomers, many solutions with various silica concentrations are prepared by dilution with acrylate. A photosensitive initiator –Irgacure from Ciba- and a cross-linker (butanedioldiacrylate) are then added to each dispersion. The polymerisation and the crosslinking reaction occur simultaneously by U.V. illumination.

Note that for every systems, the cross-linker concentration was kept equal to 0.3% per mol of acrylate monomers. The grafting density  $\Gamma$  was measured by elemental analysis and we have deduced the thickness of the layer  $e_{\text{graft}}$  composed of the grafters. The shape and the size of the particles were characterized by Small Angle Neutron Scattering (SANS) [22]. These measurements have also shown that the particle surfaces were smooth.

## **B) Samples characterization.**

The four sample sets studied in this work have been characterized by many ways [22, 25, 26]. We have summarized in this section the main results. We have taken the nomenclature used in the reference [22].

The first and the second sets referred to as MCS\_I and MCS\_II consist in cross-linked ethylacrylate chains reinforced with silica particles grafted with the 3 methacryloxy propyl dimethylchlorosilane (MCS). The samples belonging to the third set contains silica particles grafted with acetoxylethyl-dimethylchlorosilane (ACS) and are referred to as ACS. The fourth and fifth sets referred to as TPM\_III and TPM\_VI contain silica particles grafted with the 3 –trimethoxysilylpropylmethacrylate (TPM). The particles have a diameter around 50 nm except for the TPM\_III samples where the particle size is 80 nm.

The MCS and ACS grafters molecules have only one group able to react with the hydroxyl groups located at the particle surface.  $^{29}\text{Si}$  NMR measurements have shown that the MCS and the ACS grafters form brushes over the particle surface. At the opposite, the TPM molecules have three methoxy groups and form a dense and highly cross-linked shell around the particle surface.

Moreover, the MCS and the TPM molecules have a methacrylate group and can then copolymerize with the acrylate monomers during the polymerisation step. At the opposite, the ACS grafters can not form covalent bond with the monomers. The existence of covalent bond between the MCS or TPM coated particles and the elastomer matrix have been confirmed both by swelling measurements [25] and  $^1\text{H}$  NMR spectroscopy which was used to measure the total topological constraints density  $\nu_{\text{tot}}$  of each sample [24]. The average functionality  $\langle f_{\text{Si}} \rangle$  of the particles have been deduced from the  $^1\text{H}$  NMR measurements. The same analysis has confirmed that the ACS particles are not connected to the elastomer matrix.

All these measurements lead to the conclusion that the particles and the elastomer matrix, are covalently bonded for the MCS\_I, MCS\_II, TPM\_III and TPM\_VI sets. At the opposite the particles are not covalently connected to the polymer chains in the ACS reinforced samples.

The arrangement of the particles in the polymer matrix have also been characterized by SANS. The MCS\_I, TPM\_III and TPM\_VI samples have very good dispersion state i.e. the particles seem to have an exclusion shell around them and behave as repelling one another. At the opposite, we observed the presence of few linear aggregates coexisting with single particles in the MCS\_II samples while the ACS elastomers contain large fractal aggregates. These three types of dispersion will be respectively called very good, bad and very bad dispersion states in the following. All the structural features of the four sample sets are summarized in the table I.

### **C) Mechanical measurements**

The mechanical measurements were performed on a Rheometrics RDA II in simple shear strain with a plate-plate geometry. Samples were disks of 8mm diameter and 2mm thickness. They were glued with a cyanoacrylate glue (loctite) on the plates of the rheometer. Mechanical measurements were performed on a temperature range from 303K to 383K and frequencies between 0.01Hz and 10Hz. The data in the non-linear regime were measured with a deformation mode. The sample was submitted to ten deformation cycles prior the beginning of each dynamical modulus measurement. Some of the data – linear regime for sets ACS– have already been published in [13]. For the sake of comparison, the viscoelastic modulus of the matrix – crosslinked polyethylacrylate – were also performed (see ref [13]). The glass transition temperature at 1 Hz was found equal to 253K. We present now the bared data measured in the non-linear regime.

## Experimental results

In Figure 1, we have plotted the real part of the dynamical modulus variation with the strain amplitude for various samples, frequencies and temperatures. It allows to see the effect of temperature, frequency and dispersion state on the non-linear mechanical behavior of our systems.

We can first observe that the non-linear behavior of our filled samples – for the same frequency and temperature - is sensitive to the quality of the dispersion state (compare open circles in figure 1a and 1b or see data in figure 2). For samples with “very good” dispersion – MCS\_I, TPM\_III and TPM\_VI- in which the particles are surrounded by an exclusion radius, the value of the dynamical modulus remains constant for deformation up to 1 (see figure 2). But for samples having bad dispersion state, we measure a non-linear viscoelastic behavior on the same deformation range (figure 1a and 1b). The real part of the shear modulus decreases for increasing deformation amplitude while the dissipative part of the modulus goes through a maximum (data not shown). The modulus variation is larger for the very badly dispersed ACS samples than for the MCS\_II samples.



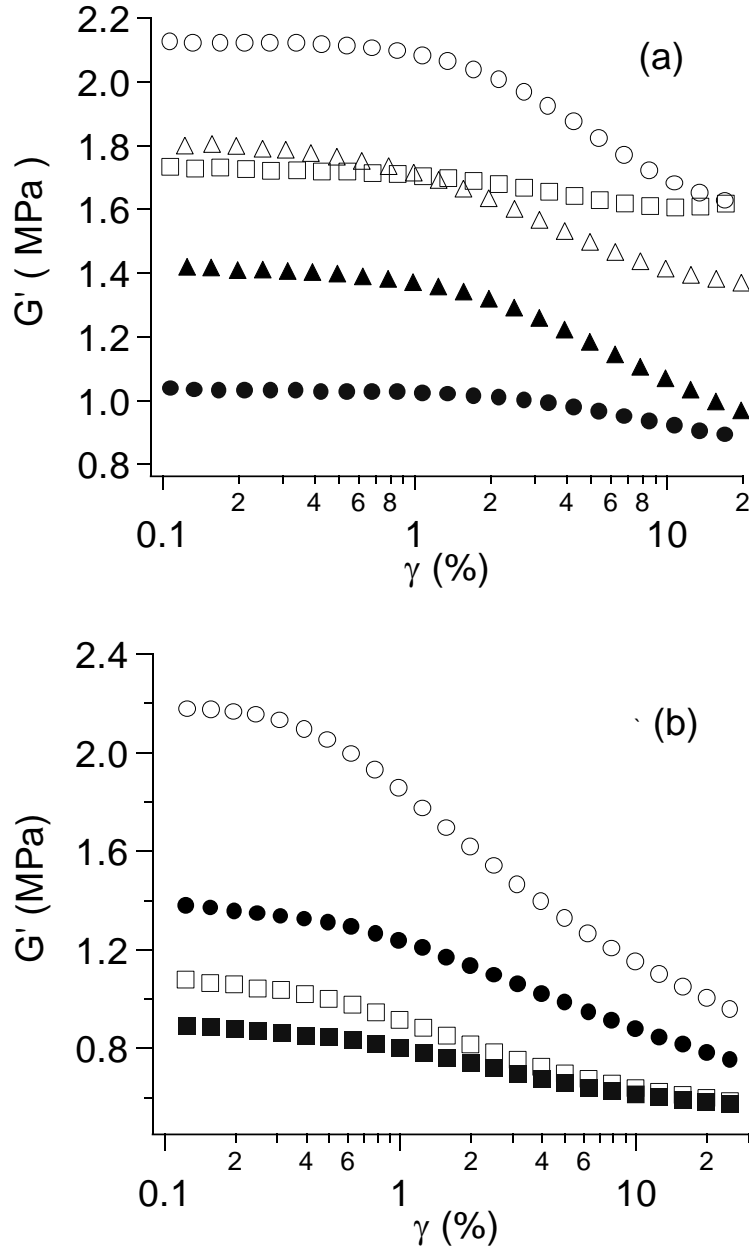


Figure 1 : Variation of the real part of the shear modulus  $G'$  versus the deformation  $\gamma$ . (a) MCS\_II samples  $\Phi = 0.21$  : (○)  $\omega = 0.1$  Hz and  $T = 303$  K , (□)  $\omega = 0.1$  Hz and  $T = 343$  K, (△)  $\omega = 0.01$  Hz and  $T = 303$  K.  $\Phi = 0.15$  : (●)  $\omega = 0.1$  Hz and  $T = 303$  K , (▲)  $\omega = 10$  Hz and  $T = 303$  K. (b) ACS samples  $\Phi = 0.18$  : (○)  $\omega = 0.1$  Hz and  $T = 303$  K , (□)  $\omega = 0.1$  Hz and  $T = 343$  K,  $\Phi = 0.15$  : (●)  $\omega = 0.1$  Hz and  $T = 303$  K , (■)  $\omega = 0.1$  Hz and  $T = 343$  K.

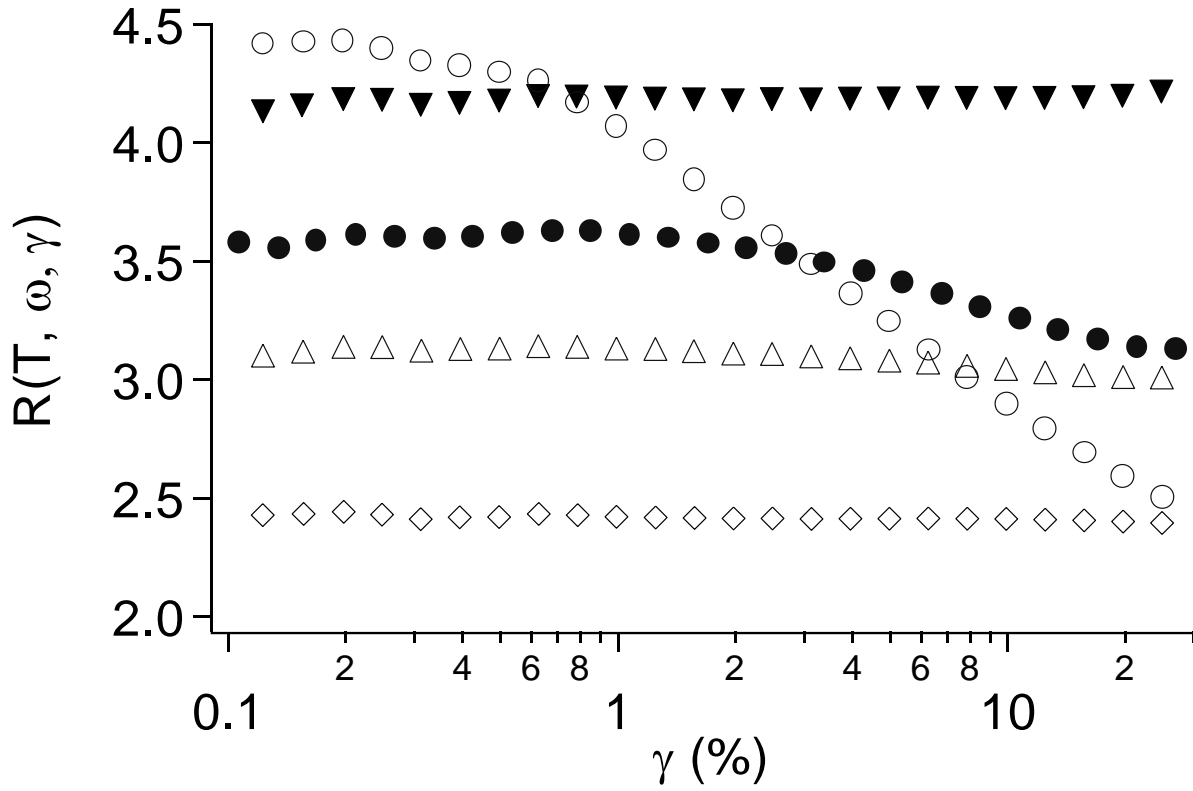


Figure 2 : Variation of the reinforcement  $R(T, \omega, \gamma)$  of MCS\_I, TPM\_VI and TPM\_III samples versus deformation at  $T=303K$  : ( $\blacktriangledown$ ) : MCS\_I with  $\Phi=0.24$  ; ( $\diamond$ ) TPM\_III with  $\Phi=0.18$ ; ( $\triangle$ ) TPM\_VI with  $\Phi=0.18$ ; ( $\bullet$ ) MCS\_II with  $\Phi=0.15$ , ( $\circ$ ) ACS with  $\Phi=0.15$ .

Moreover, the amplitude of the modulus decrease depends on temperature, on frequency and on silica concentrations. For ACS and MSC\_II sample sets, we observed the same main features. The amplitude of the dynamical elastic modulus decrease is larger as the silica concentration increases (compare open and filled circles in figure 1a or in figure 1b). In addition, it is lower at higher temperatures (compare circles and squares in figures 1a and 1b) or lower frequencies (compare open circles and triangles in figure 1a). All these effects are sharper for the ACS samples than for the MCS\_II samples.

All these features have been observed on many kind of filled elastomers undergoing an increasing dynamical deformation and is called the Payne effect. The non-linear behavior shown by our samples is consistent with those observed on other filled elastomers [11].

How can these non-linear behaviors be explained? The differences observed between the very well dispersed (MCS\_I, MP\_III or TPM\_VI) and the very bad dispersed (ACS) samples indicates that the arrangement of the particles strongly influences this non-linear behavior. However, the temperature and frequency dependence of the Payne effect shows that it does not result in purely geometrical – or hydrodynamical - effects. Hence, any interpretation must deal not only with the effects of the particle arrangements, but also with an other temperature and frequency dependent mechanism. Moreover, we observed a Payne effect with the MCS\_II samples for which the grafted silica particles are covalently bonded to the cross-linked poly(ethylacrylate) chains. An absorption/desorption picture is thus not appropriate to explain the non-linearity observed in these filled systems.

On the other hand, it is known for years that the introduction of solid particles in an elastomer matrix leads to a slowing down of the dynamics of the polymer chains located near the particle surface. The slow dynamics looks like the one of polymer chains in the glassy state [7-12]. In the following we analyze the non-linear behavior of our samples in the frame of the existence of a glass transition gradient near the particle surfaces. We first recall how the existence of a glass transition gradient modifies the mechanical properties of the filled elastomers in the linear regime. Then we extend this concept to the non-linear regime.

## **Theoretical section**

### **A) Theoretical Background: Influence of a glass transition gradient on the mechanical properties of filled elastomers in the linear regime.**

#### *A-1) Existence of a glass transition gradient near the particle surfaces*

New insights for the understanding of the dynamic modification of a molten polymer near a surface have been obtained from experiments on thin polymer films deposited on a solid substrate. Many experiments made on different systems and by different authors [14-17] have revealed that the glass transition temperature of thin polymer films is shifted compared to the one measured in the bulk. For polymer films strongly absorbed on a substrate, it has been observed that a positive shift of the glass transition temperature of the order of 30K can be observed for polymer films of 10 nm thickness. It has then been suggested that the glass transition of a polymer is shifted because of the presence of the interface. Recently, a theoretical approach has proposed an interpretation of this phenomena. According to [20], there would be a glass transition temperature gradient at the substrate surface. Let us recall briefly this approach.

The existence of a glass transition gradient near a surface is seen as a consequence of the physical origin of the glass transition. The glass transition can be naively viewed as following: thermodynamical density fluctuations result in dynamical heterogeneities, that are present in any molecular glasses, because the dynamics is extremely sensitive to the density. Thus this suggests that the glass transition would originate in the percolation of the densest - or slowest – domains. In other words, at the glass transition, the rigidity originates in the existence of a skeleton of slow domains.

As the percolation threshold varies with the sample dimensionality, the glass transition of a thin film - that corresponds to a nearly-2d geometry - should be different to the one of the bulk – 3d geometry. Moreover, the percolation threshold depends also on the interactions at the polymer /substrate interface. For polymer films strongly interacting with the substrate, the threshold is lower due to the emergence of additional rigid paths through the substrate. According to [20], the glass transition at a given frequency  $T_g^\omega$  would vary with the distance  $z$  to the substrate surface following the equation :

$$T_g^\omega(z) = T_g^\omega(1 + (\delta/z)^\nu) \quad (1)$$

where  $\delta$  is the length controlling the amplitude of the gradient,  $T_g^\omega$  is the bulk glass transition at the frequency  $\omega$ . The exponent  $\nu$  is equal to 0.88. This law is nearly similar to the one suggested by Keddie [14], and observed on polymer films when the radius of gyration of the chains is smaller than the film thickness.

The existence of such glass transition gradient was intuited by Wang [11] to be at the origin of the modification of the filled elastomers mechanical properties in the linear regime. We have recently shown [13] that this concept allows to describe quantitatively some properties of the linear dynamical elastic modulus that we will recall now.

Remark: In the following and for the sake of clarity, we sometimes omit the suffix  $\omega$ . Moreover, the notation  $T_g$  corresponds always to the bulk value of the glass transition, while  $T_g(z)$  stands for the glass transition temperature modified by a surface at a distance  $z$ .

#### *A-2) Temperature-frequency superposition for filled elastomers in the linear regime*

As described in [13], the hypothesis of the existence of a gradient of glass transition temperature near the particles allows to describe the frequency–temperature dependence of the linear mechanical properties observed on our filled elastomers for  $T$  higher than  $T_g$  ( $T > T_g + 50$ ).

Actually, the temperature of the glass transition increases for polymer at decreasing distance from the particle interfaces, following equation (1). Thus above the bulk glass transition temperature the polymer chains are in the glassy state near the particle surface and the polymer chains are in the rubbery state far from the particles. In fact, the elastic modulus varies weakly with temperature, in the two following domains,  $T - T_g(z) < -10$  K and  $T - T_g(z) > 30$  K. But it varies of at least 3 orders of magnitude for  $T - T_g(z)$  between  $-10$  K and  $30$  K. As  $T - T_g(z)$  varies strongly with the distance to the interface  $z$ , the dynamical elastic modulus varies extremely abruptly from its glassy value to its rubbery value. This allows the following coarse-grained approximation for temperature higher than  $T_g + 50$  K. We can consider that the

polymer chains for which  $T_g(z)$  is higher than  $T$  are infinitely rigid while the other ones have an elastic modulus equal to the one of the bulk polymer. Thus we can define a shell of glassy polymer around the particles which thickness  $e_g$  is given by  $T_g(e_g) = T$  and is temperature dependent. The glass transition temperature of the matrix being frequency dependent and according the equation (1), the thickness  $e_g$  will also vary with frequency. This leads to the following expression for  $e_g$  :

$$e_g(T, \omega) = \delta (T_g^\omega / (T - T_g^\omega))^{1/\nu} \quad (2)$$

Let us remark that this temperature dependence of the glassy thickness has been confirmed by NMR measurements [12,13]. The values of  $\delta$  have been measured for our samples by  $^1\text{H}$  NMR and are given in table I. According to this coarse-grained approximation, the macroscopic modulus is controlled by two parameters: the thickness of the glassy shell and the arrangement of the particle inside the matrix.

Thus *for a given sample*, i.e. a given arrangement of particles, the temperature and frequency dependence of the modulus is controlled by the variation of  $e_g$  with  $T$  and  $\omega$  according to eq. (2). The modulus of the filled sample  $G(T, \omega, \Phi)$  is then only fixed by the reduced variable  $(T_g^\omega / (T - T_g^\omega))$ . This is expected for any given sample whatever the arrangement of the particles. For instance, if glassy bridges mechanically connect pairs of particles leading to the formation of solid clusters, the morphology of these solid clusters will only depend on the reduced variable  $(T_g^\omega / (T - T_g^\omega))$ .

### *A-3) Experimental validation of this temperature-frequency superposition in the linear regime*

This theoretical prediction has been validated by the mechanical data measured on our filled samples [13]. We have shown that the reinforcement  $R(T, \omega, \Phi)$  – i.e. the modulus of the filled elastomer  $G(T, \omega, \Phi)$  divided by the one of the non reinforced matrix  $G(T, \omega, \Phi=0)$  fulfills this temperature-frequency superposition law. Let us remark that the reinforcement –instead of the bare modulus  $G(T, \omega, \Phi)$  - is used in the master curves in order to take into account the entropic behavior of the

polymer chains far from the particle. By entropic behavior we mean the increase of the elastic modulus proportional to temperature above  $T_g + 50K$ .

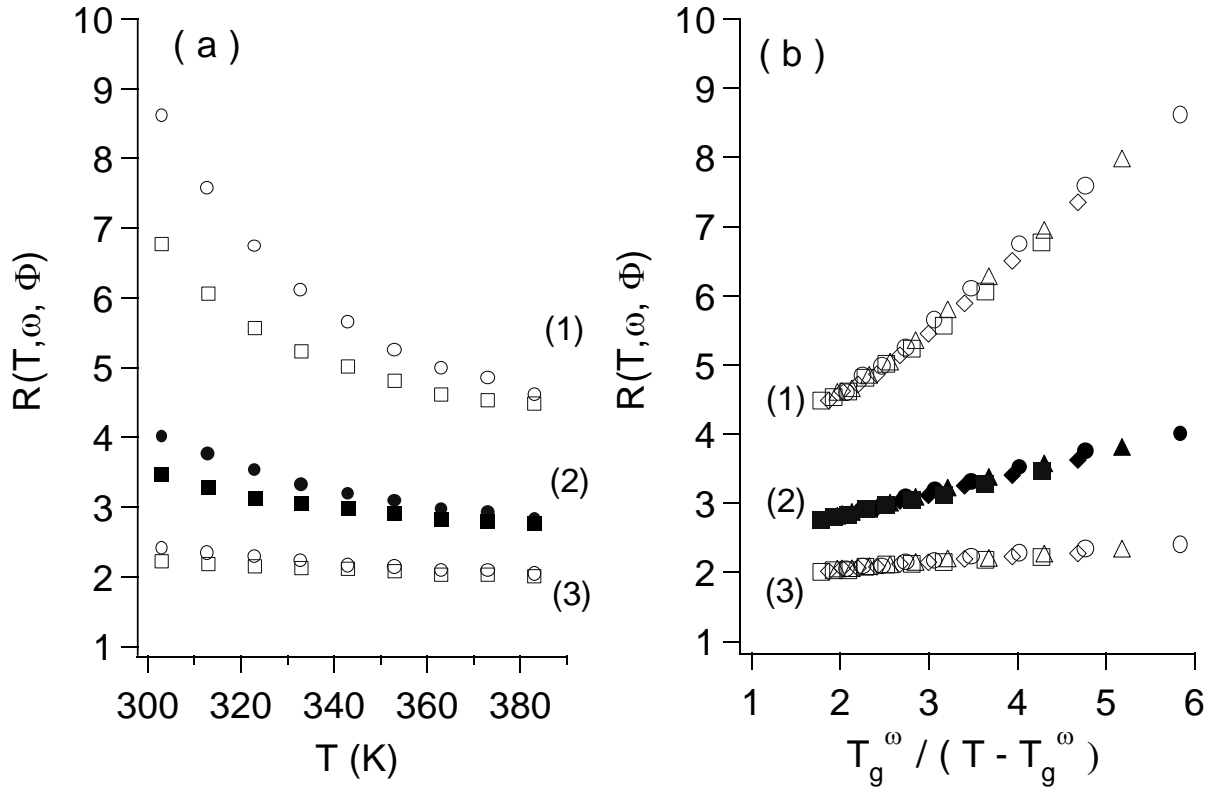


Figure 3: (a) : Variation of the reinforcement  $R(T, \omega, \Phi)$  with temperature and frequency for MCS\_II samples having varying silica concentrations. Measurements were performed in the linear regime. (1) :  $\Phi = 0.21$  , (○)  $\omega = 10$ Hz, (□)  $\omega = 0.01$ Hz; (2) :  $\Phi = 0.15$  , (●)  $\omega = 0.10$ Hz, (■)  $\omega = 0.01$ Hz; (3) :  $\Phi = 0.12$  , (○)  $\omega = 10$ Hz, (□)  $\omega = 0.01$ Hz. (b) : Shape of the master curves obtained plotting the reinforcement  $R(T, \omega, \Phi)$  versus  $T_g^\omega / (T - T_g^\omega)$ . The labels (1) , (2) and (3) correspond to MCS\_II samples containing a silica volume fraction  $\Phi$  of 0.21, 0.15 and 0.12 respectively. The frequency associated to the different data are: in circle  $\omega = 10$  Hz, in triangle  $\omega = 1$ Hz, in diamond  $\omega = 0.1$ Hz and in square  $\omega = 0.01$ Hz.

The Figure 3a shows the dependence of the reinforcement versus temperature and frequency for MCS\_II samples having varying silica concentration. The data were measured for temperature  $T$  such that  $T > T_g^\omega + 50K$  i.e. in a temperature range where the non reinforced matrix has an entropic behavior

( $G \propto T$ ). The mechanical behavior of these filled samples clearly departs from the one of the unfilled elastomer in the same temperature range.

A master curve is obtained for each concentration when plotting the reinforcement versus the reduced variable  $Tg^\omega/(T - Tg^\omega)$ , in agreement with the theoretical predictions in the linear domain (see Figure 3b).

Similar master curves were obtained with the other systems whatever their structure – dispersions states and interactions at the interface. We have shown in [13] that this is also valid for the ACS system that have very bad dispersion and weak interactions at the interface. For very well dispersed MCS\_I, TPM\_III or TPM\_VI, the temperature dependence of the reinforcement is weak (see figure 4) but visible for the highest silica concentration. Thus, the concept of glass transition gradient describes the mechanical behavior observed in the linear regime for the filled elastomers whatever the structure of the sample. Moreover, the absolute values of the reinforcement  $R$  is strongly influenced by the dispersion state. The more disordered the arrangement of particles is – i.e. the “worst” the dispersion is - the larger the slope of the reinforcement versus  $Tg^\omega/(T - Tg^\omega)$  is.

In conclusion of this part, all our filled systems verify the temperature-frequency superposition law predicted from the existence of a glass transition gradient near the particles surfaces. This result shows that:

- i) the glassy shell – already revealed by NMR or by physical aging experiments - is in fact induced by the presence of a glass transition temperature gradient near the surface
- ii) the thickness of this glassy layer depends on temperature and frequency.

Finally, its impact on the mechanical measurements is enhanced by strong particle/matrix interactions, short particle-particle distances or “bad dispersion” states.

We will now analyze how the existence of a glass transition gradient near the particle surfaces influences the non-linear behavior of the filled elastomers.



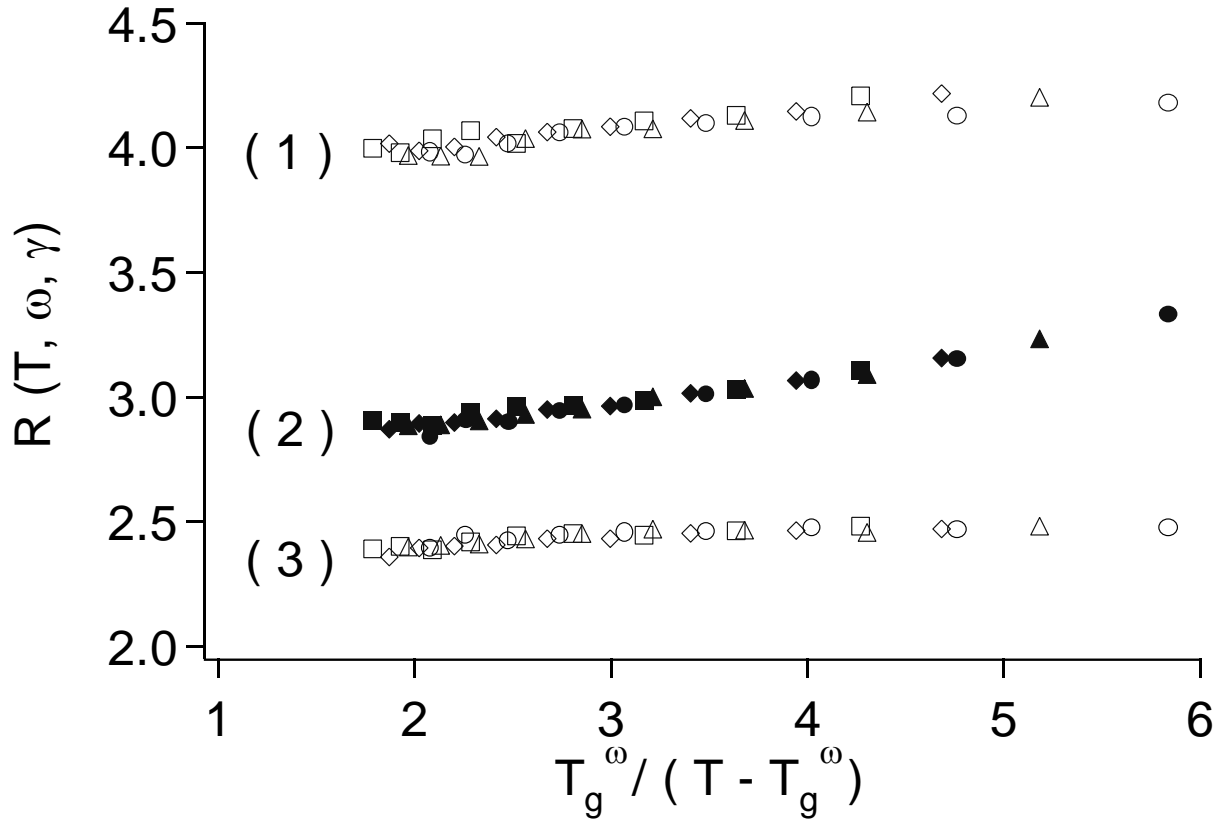


Figure 4: Variation of the reinforcement  $R(T, \omega)$  versus  $T_g^\omega / (T - T_g^\omega)$  measured on well dispersed filled elastomers in the linear regime (1) : MCS\_I with  $\Phi = 0.24$ ; (2) : TPM\_VI with  $\Phi = 0.18$ ; (3) : TPM\_III sample with  $\Phi = 0.18$ .

## B) Non-linear viscoelastic behavior of filled elastomers: strain-softening of the glassy shells.

In this section we will first assume that the glassy shell surrounding the particles surfaces can undergo a strain softening under a large cyclic deformation, similarly to what is observed for a bulk polymer. We will then estimate the consequences of this assumption for the non-linear mechanical properties of filled rubbers. We will then compare our experimental results with our prevision. Let us first recall the main features of the non-linear behavior of a bulk glassy polymer undergoing a cyclic deformation.

### B-1) Non-linear behavior of a bulk glassy polymer: strain softening under cyclic deformation

Despite the complexity of non-linear mechanics of solid polymers, we aim to describe it quite naively, in order to estimate its consequences for filled rubber. Therefore, we will limit ourselves here to a very schematic description of solid polymer mechanics. The conventional stress-strain curve of a glassy polymer undergoing an unidirectional loading is composed of three distinct regions [27]. In the first domain, the true stress  $\sigma$  increases nearly linearly with the strain  $\gamma$  up to the yield point characterized by its deformation  $\gamma_y$  and its yield stress  $\sigma_y$ . Beyond the yield point there is a fall in true stress such that the ratio  $\sigma/(G_g\gamma)$  decreases as the deformation increases ( $G_g$  is the elastic modulus in the glassy state). It varies typically from 1 to  $5 \cdot 10^{-2}$  for a strain varying from 0% to 50%. This is commonly known as the strain-softening regime and is observed from the yield point up to a deformation referred to as  $\gamma_l$ . Finally for deformations larger than  $\gamma_l$ , the ratio  $\sigma/(G_g\gamma)$  increases again but remains lower than 1 in this last regime.

The values of the yield stress and of the yield deformation are temperature dependent: both increase for decreasing temperature. Actually at a given loading rate the yield stress  $\sigma_y$  varies linearly with temperature according to the well-known empirical relation [24, 25, 28, 29]:

$$\sigma_y \sim K_y (T_g - T) \quad (3)$$

where  $K_y$  is of the order  $1 \text{ MPa K}^{-1}$ .

Moreover, the stress-softening observed beyond the yield point is attributed to the growing up of some rubber-like domains under the loading by many authors. They have shown that a strain-softened glassy polymer is constituted by rubber-like domains embedded in a glassy matrix [30,31].

What happens now if a cyclic instead of a monotonic deformation is applied to a bulk glassy polymer? Under cyclic deformation, after a few cycles, the mechanical response becomes stable and apparently linear. By *apparently linear* we mean that,

-under a sinusoidal deformation, the response contains mostly only the frequency  $\omega$  component of the excitation, while the amplitudes for frequencies  $n\omega$ , where  $n$  is an integer larger than 1, are nearly zero  
- but simultaneously, the response amplitude is not proportional to the amplitude of the solicitation.

Thus the glassy polymer is characterized by an apparent modulus  $G_{ap}$ . This modulus strongly decreases with the strain amplitude. It decreases from its linear value  $G_g$  to values even lower than the ratio  $\sigma/\gamma$  measured on the unidirectional test – this phenomena being called cyclic softening [32-33]. Moreover, this phenomena is both temperature and frequency dependant.

This observation is reminiscent to the one made by Chazeau et al [34] on filled rubbers. These authors have shown that, after several deformation cycles of same amplitude, the response of the filled elastomer becomes stationary and almost purely sinusoidal as observed for glassy polymers undergoing a large cyclic deformation. Thus the assumption that a part of the glassy shells undergoes a cyclic-softening after a few cycles of a large cyclic deformation is perfectly consistent with the observations made both on filled elastomers and glassy bulk polymer.

But let us precisely now introduce our assumption for the strain-softening of the glassy polymer shell.

## *B-2) consequences for filled elastomers*

### *Hypothesis for the strain-softening in filled rubber*

First let us claim that as for monotonic loading, the strain-softening of bulk polymers for cyclic-softening test originates in the formation of small domains with a rubber-like modulus.

Here we are dealing with cyclic strain-softening of very thin layers of glassy polymer. It is thus reasonable to assume that nanometric polymer films that are strain-softened behave as the rubber-like domains in bulk polymer during cyclic softening.

We can then deduce how the glassy shells can be partly strain-softened as an increasing cyclic deformation is applied to the filled elastomer. We assume here that the glassy polymer chains located at

the distance  $z$  from the neighboring particle surface behaves under a cycle of amplitude  $\sigma$ , of frequency  $\omega$ , at temperature  $T$  and in the stationary regime, with the following characteristics:

- i) for  $\sigma < \sigma_y$  their apparent modulus  $G_{ap}$  is of the order of  $G_g$
- ii) for  $\sigma > \sigma_y$  their apparent modulus  $G_{ap}$  is of the order of the matrix modulus in its rubber state.
- iii) their yield stress  $\sigma_y$  is given by  $K_y(T_g(z) - T)$

This last assumption combined to the existence of a glass transition gradient leads to the existence of a gradient of yield stress around the particles. The spatial distribution of the yield stress can be expressed using equations (1) and (3) as:

$$\frac{\sigma_Y(z)}{T_g^\omega} = K \frac{T - T_g^\omega}{T_g^\omega} \left( 1 - \frac{T_g^\omega}{T - T_g^\omega} \left( \frac{\delta}{z} \right)^{1/\nu} \right) \quad (4)$$

We now examine the consequences of these assumptions on the mechanics of filled elastomers.

#### *consequences for isolated particles in a matrix*

In this section, we consider the case of a single particle surrounded by a polymer matrix. This case is representative of filled elastomers such that all the particles are well separated from their neighbors, as in a colloidal crystal, and such that, in the considered temperature range, there are no glassy bridges between particles. This is commonly identified as a sample with “a very good dispersion state”.

Now, let's apply a macroscopic stress  $\Sigma$  to the sample. Because of the heterogeneities of the system the stress is redistributed in a stress field  $\sigma(\mathbf{r})$  where  $\mathbf{r}$  is the position in the sample. But in the case of isolated particles, one can show that – assuming an incompressible elastomer – the ratio between the local and the macroscopic stress remains between 0 and 5/2 [36]. Thus this stress redistribution is weak

in this case. However the polymer matrix such that  $\sigma(\mathbf{r}) = \sigma_Y(z(\mathbf{r}))$  undergoes a plastic deformation leading to their strain-softening. Here  $z(\mathbf{r})$  is the distance between the point  $\mathbf{r}$  and the nearest interface.

Thus, this strain-softening leads to a decrease of the apparent modulus of the polymer chains located at a distance  $z$  such that  $\sigma_Y(z(\mathbf{r})) = \sigma(\mathbf{r})$ .

In the case of a single particle, there is thus an about isotropic strain-softening of the glassy layer around the particle. If we assume, like in [13] that the modulus of the non-softened glassy polymer chains is infinitely rigid – as compared to the polymer in the rubber or strain-softened state, the coarse-grained approximation is then straightforward. In this frame, we can then express the variation of the thickness of the glassy polymer layer  $e_g$  with the local stress  $\sigma$ . Moreover, the local stress  $\sigma$  is approximately equal to the macroscopic one  $\Sigma$  as the particles are isolated. We can thus defined the thickness  $e_g(\Sigma)$  at temperature  $T$  such that the polymer chains located at  $z > e_g$  are either in the rubber state or strain-softened. This corresponds to the following:

$$T_g(e_g(\Sigma)) - \Sigma/K_y \approx T \quad (5)$$

leading to the relation

$$e_g(\Sigma) \approx \delta (T_g^\omega / (T - T_g^\omega + \Sigma/K_y))^{1/\nu} \quad (6)$$

Hence, the thickness of the glassy layer decreases for increasing stress amplitudes. However, this equation is valid only if the stress is nearly homogeneous, and thus for large distances between particles. But in general the distance between particles is widely distributed and the local stress can be very different from the macroscopic one.

### *Real filled systems*

In a real system, the distance between two particle surfaces is widely distributed and glassy bridges eventually connect pairs of neighboring particles, or even clusters. The existence of glassy bridges between particles leads to a strongly heterogeneous distribution of the stress field within the sample that complicates the response of a real filled system compared to the one with isolated particles. Indeed, the

stress distribution in the sample is very sensitive to the morphology of the rigid inclusions formed by the particles and the glassy bridges connecting them. Hence, if we assume that part of the glassy phase is strain-softened as a large macroscopic deformation is applied, the morphology of the rigid inclusions changes leading to a redistribution of the stress within the sample.

In a Payne experiment, for each deformation amplitude, few deformation cycles are applied before the modulus measurement is performed. It results that the scenario for the macroscopic strain-softening is quite complex. During the first deformation cycle, the polymer chains such that  $\sigma(\mathbf{r}) = \sigma_Y(z(\mathbf{r}))$  are strain-softened. This partial strain-softening leads to new stress distribution in the sample such that during the following deformation cycles of the same amplitude, new glassy polymer chains are strain-softened. This progressive strain-softening of a part of the glassy layers continue until a state is reached where all the domains where  $\sigma(\mathbf{r}) = \sigma_Y(z(\mathbf{r}))$  are strain-softened -  $\sigma(r)$  depending itself on the strain-softened domains geometry. The filled elastomer reaches then a stationary response that is “apparently linear” – similarly to cyclic-softened bulk polymer - as observed by Chazeau et al [34].

At least for each amplitude variation, a new state of this complex strain-softening arrangement is reached.

To summarize, in the frame of our assumption an increasing macroscopic stress leads to a strain-softening of the glassy polymer shells. Thus it results in a decrease of the glassy polymer volume and finally of the dynamical elastic modulus, but the response remains purely sinusoidal – i.e “apparently linear”. This allows to explain qualitatively the Payne effects observed in reinforced elastomers. We will see now that despite its complexity the Payne effect may exhibit – in the frame of our assumption- some specific properties. First, we predict a frequency-temperature superposition in the linear regime. Secondly we will be able to discuss the respective effects of the stress amplitude and the temperature on the morphology of the glassy shell.

### *B-3) Master curves for the non-linear elasticity of filled elastomers.*

In the non-linear regime, the morphology of the solid inclusions depends on both the reduced variable  $T_g^\omega/(T-T_g^\omega)$  and the spatial distribution of the yield stress given by equation (4). The non-linear variation of the dynamical modulus only depends on the arrangement of the glassy shell which is determined by the equation  $\sigma_y(z(\mathbf{r})) = \sigma(\mathbf{r})$ . Because the local yield stress divided by  $T_g^\omega$  is a function of the reduced variable  $T_g^\omega/(T-T_g^\omega)$  alone (as shown in equ. (4)), we can assert the following law : for a given sample and at a given value of  $T_g^\omega/(T-T_g^\omega)$ , the non-linear dynamical modulus will depend only on  $\Sigma / T_g^\omega$  where  $\Sigma$  is the macroscopic stress applied to the sample.

Finally, this means that for a given sample, i.e. a fixed particle dispersion state, the reinforcement  $R(T, \omega, \Sigma)$  is only a function of two parameters:  $\Sigma/T_g^\omega$  and the variable  $T_g^\omega/(T-T_g^\omega)$ . Let us remind that this new non-linear law is only valid in the frame of our coarse grained approximation, i.e. in the approximation of an infinite mechanical contrast between glassy polymer and rubber or strain-softened polymer. This approximation fails if  $T < T_g + 50K$ .

In Figure 5-a, we have plotted the dynamical modulus, divided by its value at vanishing amplitude, as a function of the stress amplitude divided by  $T_g^\omega$ , for a MCS\_II sample containing 0.21 (vol) silica particles. This plot has been performed for two values of  $T_g^\omega/(T - T_g^\omega)$  : 3.783 and 2.464 . At a fixed  $T_g^\omega/(T - T_g^\omega)$  all the data superimpose on a master curve. But the shape of the master curve changes with the value of  $T_g^\omega/(T - T_g^\omega)$  . Similar results were obtained with the ACS sample having a silica volume fraction of 0.18 (see figure 5-b).

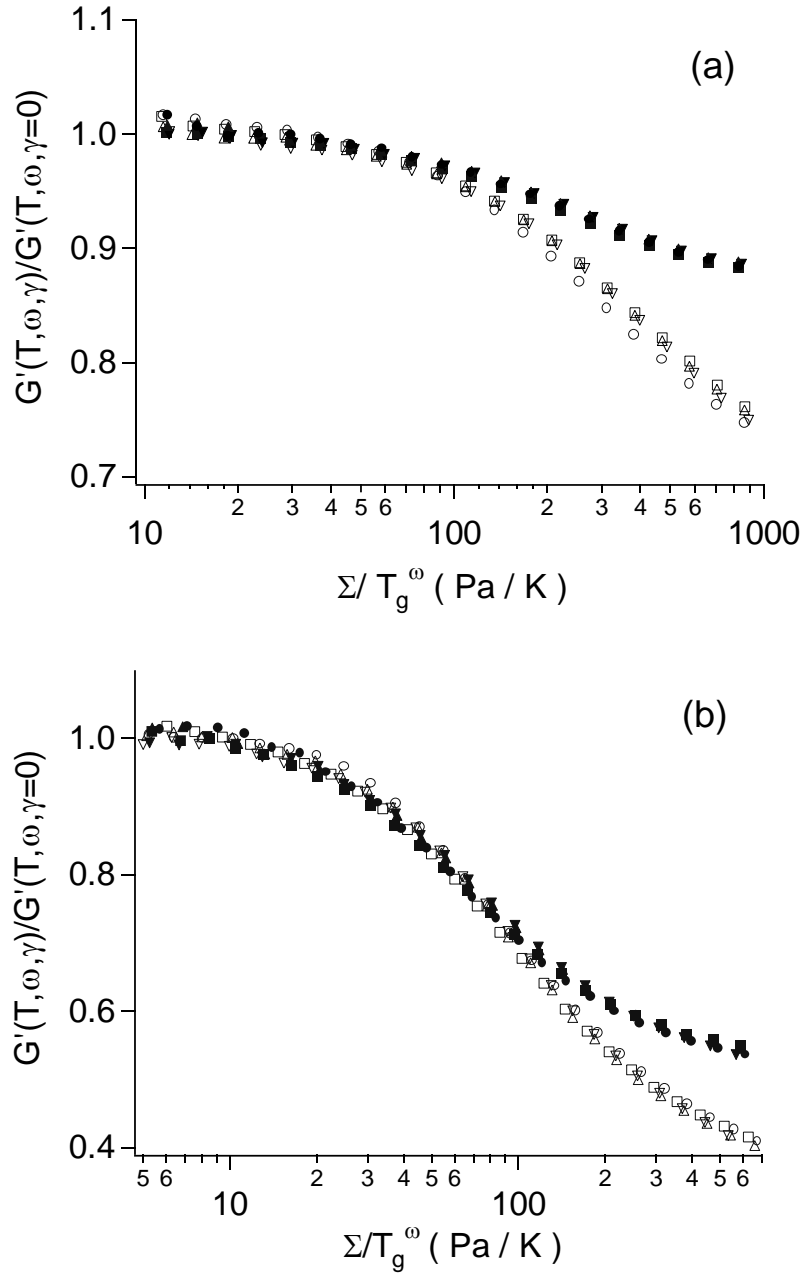


Figure 5: Master curves showing the dependence of the normalized real part of the shear dynamical modulus  $G'(T, \omega, \gamma)/G'(T, \omega, \gamma=0)$  on the deformation  $\gamma$  at constant  $T_g^\omega/(T-T_g^\omega)$ . (a) : MCS\_II sample with  $\Phi=0.214$ .  $T_g^\omega/(T-T_g^\omega) = 3.783$  : (○)  $\omega = 0.01\text{Hz}$  and  $T=308.5\text{K}$ , (□)  $\omega = 0.1\text{Hz}$  and  $T=314\text{K}$ , (△)  $\omega = 1\text{Hz}$  and  $T=319.5\text{K}$ , (▽)  $\omega = 10\text{ Hz}$  and  $T=325\text{K}$ .  $T_g^\omega/(T-T_g^\omega) = 2.464$  : (●)  $\omega = 0.01\text{Hz}$  and  $T=343\text{ K}$ , (■)  $\omega = 0.1\text{Hz}$  and  $T=348.5\text{ K}$ , (▲)  $\omega = 1\text{Hz}$  and  $T=354\text{ K}$ , (▼)  $\omega = 10\text{ Hz}$  and  $T=359.5\text{ K}$ . (b) : ACS sample with  $\Phi=0.18$ .  $T_g^\omega/(T-T_g^\omega) = 3.783$  : (○)  $\omega = 0.01\text{Hz}$  and  $T=308.5\text{K}$ , (□)  $\omega = 0.1\text{Hz}$  and  $T=314\text{K}$ , (△)  $\omega = 1\text{Hz}$  and  $T=319.5\text{K}$ , (▽)  $\omega = 10\text{ Hz}$  and  $T=325\text{K}$ .  $T_g^\omega/(T-T_g^\omega) = 2.464$  : (●)  $\omega = 0.01\text{Hz}$  and  $T=343\text{ K}$ , (■)  $\omega = 0.1\text{Hz}$  and  $T=348.5\text{ K}$ , (▲)  $\omega = 1\text{Hz}$  and  $T=354\text{ K}$ , (▼)  $\omega = 10\text{ Hz}$  and  $T=359.5\text{ K}$ .



These results show that the dynamical modulus of a given reinforced sample in the non-linear regime depends – as expected in the frame of our assumptions - only on the quantities  $\Sigma/Tg^\omega$  and  $Tg^\omega/(T - Tg^\omega)$ . It shows that similarly to the value of the linear elastic modulus, the value of the non-linear modulus in the Payne regime only depends on the glass transition gradient arrangement in the sample. It thus evidences that the decrease of the modulus observed for increasing deformation amplitude (or stress amplitude) results from the strain-softening of the glassy shell in our systems. It thus confirms the validity of our hypothesis: the Payne effect originates in the strain-softening of the glassy polymer, their glassiness being induced by the existence of a gradient of  $Tg$ . In addition, as expected, the shape of  $R(\Sigma/Tg^\omega, Tg^\omega/(T - Tg^\omega))$  varies with the dispersion state of the samples. We will discuss this point in the next section.

## Discussion

### A) Strain-softening of the glassy shell at the origin of the Payne effect.

We have recently shown that the linear viscoelastic behavior of our filled elastomers is governed by the glass transition gradient near the particle surface combined with the particles arrangement within the elastomer matrix. If an increasing sinusoidal stress is applied to a reinforced system, its dynamic modulus decreases while the modulus of the non-reinforced matrix remains constant. The stress-dependence of the modulus depends both on temperature and frequency. We showed in this work that for a given sample this non-linearity of the dynamic modulus is controlled by the initial thickness of the glassy shell  $e_g^0$ , and by the amplitude of the mechanical solicitation. Thus the strain-softening of the

glassy shell surrounding the solid particles is responsible for the Payne effect in our case. Moreover, the amplitude of the Payne effect is governed by the arrangement of the particles in the sample, as discussed now.

In the well dispersed MCS\_I and TPM\_III samples we did not succeed to detect any non-linear viscoelastic behavior for deformation amplitude lower than 1. For these samples the distances between particles surfaces - typically between 10 and 60 nm depending on the silica concentration - are larger than the expected glassy layer thickness - about 3 nm at  $T_g+50K$ . On the opposite, we observe Payne effect with MSC\_II and ACS samples that contain aggregates *i.e.* in which a part of the distances between particles are lower than  $e_g$ . Thus, we observe experimentally that the strain-softening of non-overlapping glassy shells requires higher macroscopic stress than the strain-softening of glassy bridges. The absence of Payne effect in well-dispersed samples is consistent with our estimations. If we assume that the local stress is about the macroscopic stress, using eq. (6), we can estimate that a decrease of the glassy shell from 3 nm to 2 nm requires a strain amplitude of 10! Thus the strain softening process around isolated particles is negligible. Finally, this proves that the non-linear behavior of  $G'(\Sigma)$  is mainly controlled by the strain-softening of the glassy bridges connecting solid particles. We will come back to this point later on.

## **B) Slow dynamic in the non-linear viscoelastic behavior of filled elastomers**

The concept of the glassy polymer shell explains also the modulus recovery observed after the application of few cycles of a large deformation. After the cessation of the sinusoidal deformation, one observes a logarithmic drift of the linear dynamical elastic modulus [34, 35] and we have also observed the phenomena on our samples – data not shown here. The elastic modulus increases logarithmically until it reaches its initial value measured on the sample in the linear regime [34, 35]. Such a slow structural drift of the mechanical properties of a filled elastomer have also been observed by Struik, but after a temperature quench [7,8]. We suggest here that the concept of glass transition gradient around the

particles could explain qualitatively not only the Struik [7,8] experiments but also the one of Chazeau et al [34]. Both correspond to a slow evolution of the system, with a behavior similar to the one of the aging of glassy polymers, except that in the last case, the temperature jump is replaced by the cessation of a mechanical loading. It is also known that after a mechanical loading cessation the properties of a glass polymer below its  $T_g$  exhibit an aging like behavior [7]. Finally, we suggest that the logarithmic drifts observed after sollicitation in filled elastomers are simply a consequence of the aging of the glassy shells.

### **C) Equivalence between strain amplitude and temperature in filled elastomers**

#### *C-1 Comparison of effects of strain and temperature*

We have shown that the glass transition gradient is at the origin of both the decrease of the modulus with temperature in the linear regime and with the strain amplitude in the non-linear regime. In the both cases, the modulus decrease is associated to the decrease of the glassy polymer volume within the sample. However, the effect of the macroscopic deformation should not be identical to the one of temperature because the temperature decreases homogeneously the glassy shell thickness, whether the strain-softening remains localized in the domains where the local stress is the largest. Indeed, the reinforcement dependence with the amplitude of the macroscopic deformation  $\Gamma$  is closely related to the way the glassy domains soften under the local stress. For instance the shape of  $R(\Gamma)$  is different according to whether there are glassy bridges or no within the sample. It results that the strain-softening of a given domain of glassy polymer should occur at different strain amplitudes whether it is located within a glassy bridge or not. At the opposite, a temperature increase induces an homogeneous decrease of the glassy polymer volume within the sample. Thus a comparison of the strain and the temperature roles should give a deeper insight about the mechanisms controlling the modulus decrease, particularly in the non-linear regime.

For that aim, we compare now the dependence of the reinforcement with the stress amplitude – at temperature  $T_0$  – and the one with the quantity  $K_y(T-T^0)$  – in the linear regime. We have plotted on the same graph the variations of the reinforcement as a function of temperature in the linear regime and as a function of stress at the temperature  $T_0$ . Figure 6-a and 7-a show the data measured on a MCS\_II sample ( $\Phi = 0.20$ ) and a ACS sample ( $\Phi = 0.18$ ) respectively. The temperature dependence of the reinforcement will be called  $R_{T_0,T}$ . The temperature is rescaled in stress unit using the relation  $K_y(T-T_0)$  where  $K_y$  was taken equal to  $1 \text{ MPa K}^{-1}$  and  $T_0$  is the initial temperature. The stress dependence of the dynamical modulus measured at  $T_0$ ,  $R_{T_0,\Sigma}$  is directly plotted on the figures 6a and 7a. Each pair of curves ( $R_{T_0,T}$ ,  $R_{T_0,\Sigma}$ ) corresponds to a given initial temperature and thus merges at zero stress. In order to compare stress and temperature effects on reinforcement, it is convenient to define the function  $A(\Sigma)$  which is the multiplicative factor applied to the stress such that  $R_{T_0,\Sigma}(A(\Sigma)\Sigma)$  superimposes to  $R_{T_0,T}(K_y(T-T_0))$ .

Figures 6b and 7b show the variation of  $A$  with  $\Sigma$  determined from the comparison of the curves presented on figure 6a and 7a. We observed that  $A$  goes through a maximum as the macroscopic stress amplitude increases. We will referred as  $A^{max}$  and  $\Sigma^{max}$  the amplitude of  $A$  at its maximum and the corresponding value of  $\Sigma$ . In order to clearly visualize the position of this maximum on the  $R_\Sigma$  curves we have pointed out the position of the maximum on the figures 6a and 7a for all the temperatures  $T_0$ . This maximum corresponds to a decrease of the reinforcement of respectively about 80% and of 50% for the MCS\_II and the ACS samples. The values of  $A$  are sensitive to temperature. For both the systems,  $\Sigma^{max}$  decreases and  $A^{max}$  increases with temperature. But the temperature dependence of the parameter  $A$  is strongly influenced by the particle dispersion state with a stronger sensitivity for the worse dispersion states. Actually, the absolute value of  $A$  and its variation with  $\Sigma$  are also extremely sensitive to the dispersion state. The values of  $A$  measured on the ACS samples (see figure 7-b)- very bad dispersion state - are 10 times larger than the ones obtained from the MCS\_II samples (see figure 6-b)-bad dispersion state.

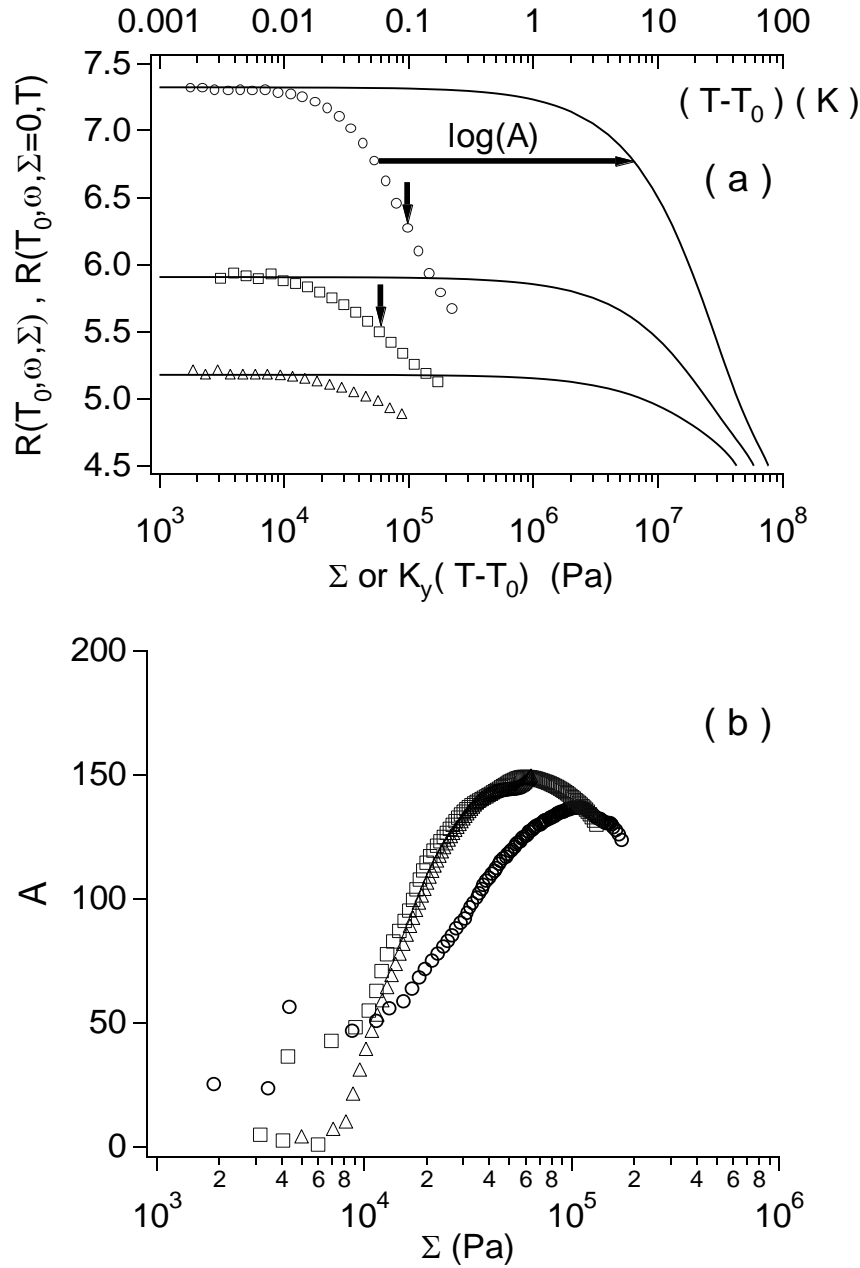


Figure 6: Comparison of the effect of macroscopic stress and temperature on the value of the reinforcement of a MCS\_II sample having the silica volume fraction of 0.214. (a) The curves showing the temperature dependence of the reinforcement  $R_T$  versus  $K(T-T_0)$  are plotted in solid lines ( $K_y = 1 \text{ MPa K}^{-1}$ ). The variation of the reinforcement with the macroscopic stress  $\Sigma$  are plotted in markers :  $T = 303\text{K}$  (○),  $T = 323\text{K}$  (□) and  $T = 343\text{K}$  (△). (b) Variation of the parameter  $A$  with the macroscopic stress  $\Sigma$  for three temperatures :  $T = 303\text{K}$  (○),  $T = 323\text{K}$  (□) and  $T = 343\text{K}$  (△). The arrows on figure 6-a point out the position of the maximum of  $A$  observed on the figure 6-b.

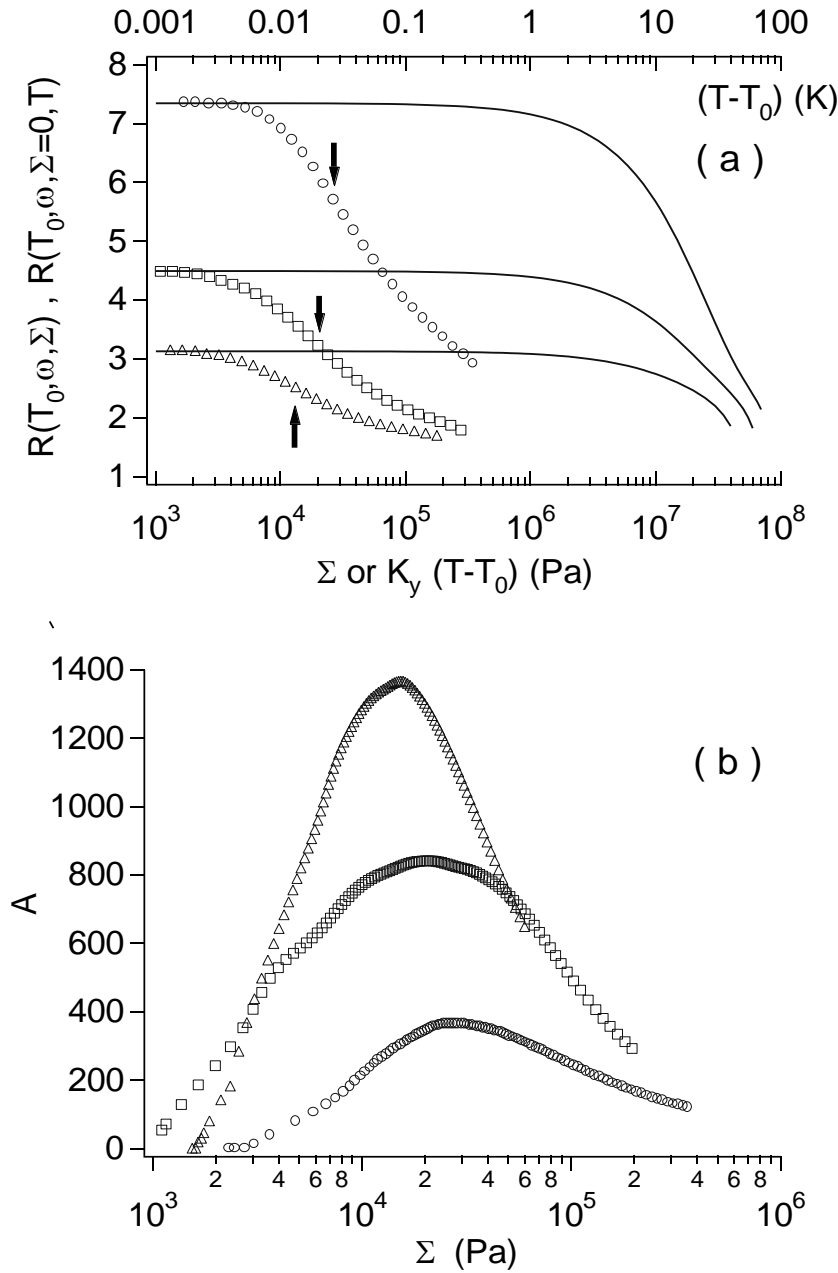


Figure 7: Comparison of the effect of macroscopic stress and temperature on the value of the reinforcement of a ACS sample having the silica volume fraction of 0.18. (a) The curves showing the temperature dependence of the reinforcement  $R_T$  versus  $K(T-T_0)$  are plotted in solid lines ( $K_y=1 \text{ MPa K}^{-1}$ ). The variations of the reinforcement with the macroscopic stress  $\Sigma$  are plotted in markers :  $T = 303\text{K}$  ( $\circ$ ),  $T = 323\text{K}$  ( $\square$ ) and  $T = 343\text{K}$  ( $\triangle$ ). (b) Variation of the parameter  $A$  with the macroscopic stress  $\Sigma$  for three temperatures :  $T = 303\text{K}$  ( $\circ$ ),  $T = 323\text{K}$  ( $\square$ ) and  $T = 343\text{K}$  ( $\triangle$ ). The arrows on figure 7a point out the position of the maximum of  $A$  observed on the figure 7b.

Let us remark that in the case of isolated particles where the local stress is nearly equal to the macroscopic one, the quantity  $A$  is expected to be constant and nearly equal to 1 but is actually very difficult to estimate by experiment

### *C-2) Physical meaning of parameter $A$ .*

Let us now comment the figures 6b and 7b. The parameter  $A$  exhibits a pronounced maximum as a function of the stress amplitude. We will try now to understand this effect in the frame of our glassy shell strain-softening approach. At first view, the parameter  $A$  can be considered as the amplification factor between the local stress and the average stress, in the glassy domains that are strain-softened. In fact,  $A$  is the average stress amplification, the average being performed on the local stress supported by the glassy domains that are strain-softened at a given amplitude. The strain-softened domains are obviously the one that supports most of the stress before the strain-softening, and the quantity  $A$  reflects the average amplification factor on the domains supporting the highest stress.

$A$  is not easy to estimate, as it combines very local stress amplification – in bridges – and amplification over the size of aggregates composed of particles connected by glassy bridges. Let us here focused on this second effect.

In order to discuss more precisely this feature, let us first introduce here a hand waving argument that allows to compare temperature versus stress amplitude decrease of the elastic modulus. Let us consider a reinforced elastomer sample containing spherical particle as follows. We take all the pairs of neighboring particles. We will call "bonds" the set composed of two neighboring particles and the polymer matrix connecting them. All the bonds constitute a network, and each bond of the network has a specific elasticity and yield stress that depend on the distance between the particles surfaces, on temperature and on the local stress. We can make the approximation that there is in fact two types of bonds, either glassy or rubber-like. The number of glassy –and thus rigid- bonds will depend on temperature and stress amplitude. We will also assume that the mechanical behavior of the sample is

roughly the one of the network. Now when we increase the temperature from the glass transition temperature of the bulk  $T_g$ , we progressively decrease the number of rigid bonds, by melting progressively the glassy polymer between the pair of particles. This decrease depends just on the distance distribution between pairs of particles. If on the contrary we increase the stress amplitude, we will strain-soften progressively the glassy bonds, depending not only on their length (distances between the two particles surfaces) but also on their local stress. Thus the ratio between the strain-softening and the temperature decrease of glassy bonds, the factor  $A$  in our case, is nearly the amplification factor of the local stress carried by the bonds that are strain-softened. In the following we will assume that the factor  $A$  is about the stress-amplification factor that we have in our sample.

Now let us discuss the evolution of the amplification factor  $A$  versus temperature and stress amplitude.

Let us recall that in our bond-network picture, increasing the temperature for a given sample, starting from  $T_g$ , one progressively melts the glassy bonds. Thus the network of glassy bonds will reach a percolation threshold at some temperature  $T_C$ . As a consequence, the amplification factor will be weak just above  $T_g$  and for very high temperature as drawn in figure 8 and it will exhibit a maximum at  $T_C$ . The amplitude at the maximum, and  $T_C$  will depend on the arrangement of the particles. If the arrangement is quite regular – crystalline for instance – the amplification factor will remain around 1. But if the system is more disordered the amplification factor will exhibit a sharper maximum.

The effect of the stress now can be compared in detail. A small temperature increase will soften bonds corresponding to a given distance between the particles surfaces, and thus a given yield stress. This distance corresponds to the longest bridges that have not yet been melt. At the opposite, a small stress increase will strain-soften the bonds where the local stress is equal to the yield stress. In this last case, the most constrained glassy bridges will be preferentially softened.

As a consequence, an increase of temperature or stress is not equivalent for stress distribution in the system. From a rigid/soft bonds ratio  $r_1$  at rest, we can reach a ratio  $r_2$  lower than  $r_1$  either by a temperature increase or by a stress increase (from right to left in fig.8). However, the amplification factor at  $r_2$  will depend on the followed path. It will be smaller in the case of stress increase than in the



case of a temperature increase, because any stress increase redistributes the stress more homogeneously than it was previously. This is schematically described in figure 8. The solid line represents the amplification factor at zero stress for various increasing the ratio of glassy bonds, or decreasing the temperature towards  $T_g$ . Obviously this is valid for a given sample but the shape of the curve will vary from sample to sample depending on anchorage between filler and matrix, volume fraction and arrangement of the fillers, nature of the polymer matrix etc... However, a bell-like shape of the curve is always expected, whatever the sample. Let us plot the amplification factors at constant temperature, increasing the stress amplitude for respectively temperature  $T_1$  and  $T_2$  (in dashed line). The dashed line has to be below the solid one, as – see above – a stress amplitude increase decreases the stress localization. Hence, the maximum of the amplification factor at  $T_1 > T_2$  is larger from  $T_1$  than for  $T_2$ . Moreover, the stress at which the amplification factor is maximum is smaller for  $T_1$  than for  $T_2$ , because there are less bonds to strain-soften to reach the maximum of  $A$ .

Let us summarize the results of this naive approach :

- i) we expect a bell-like shape for  $A$ , that originates in a maximum of stress localization, corresponding to the percolation threshold for the glassy bonds network.
- ii) we expect that the amplitude  $A^{max}$  will depend on the disorder of the particles arrangement. Characterizing the amplification factor, it must increase with the reinforcement in the linear regime, at a constant filler density and a similar polymer matrix.
- iii) we expect that the amplitude  $A^{max}$  increases with temperature, and simultaneously that the stress  $\Sigma^{max}$  decreases with temperature.

Actually, the three behaviors are observed in our samples. First all the variations of  $A$  with the stress amplitude (see figure 6a and 7a) exhibit a maximum. Secondly, the value at the maximum of  $A$ ,  $A^{max}$  is larger for ACS than for MCS\_II (compare 6b and 7b). Lastly  $A^{max}$  increases with temperature while  $\Sigma^{max}$  decreases (see in fig. 7b). Thus the factor  $A$ , even if it is probably not exactly the local stress amplification factor, describes an amplification of the local stress. Finally, a network picture is able to connect the bell-like shape of the  $A/\Sigma$  curves, the network being constituted by glassy bridges and elastic

bridges between neighboring particles. Moreover, confirming the model, the temperature variation of  $A^{max}$  and of  $\Sigma^{max}$  qualitatively agree with our experimental results, confirming once again the picture of a glassy polymer shell around each particle.

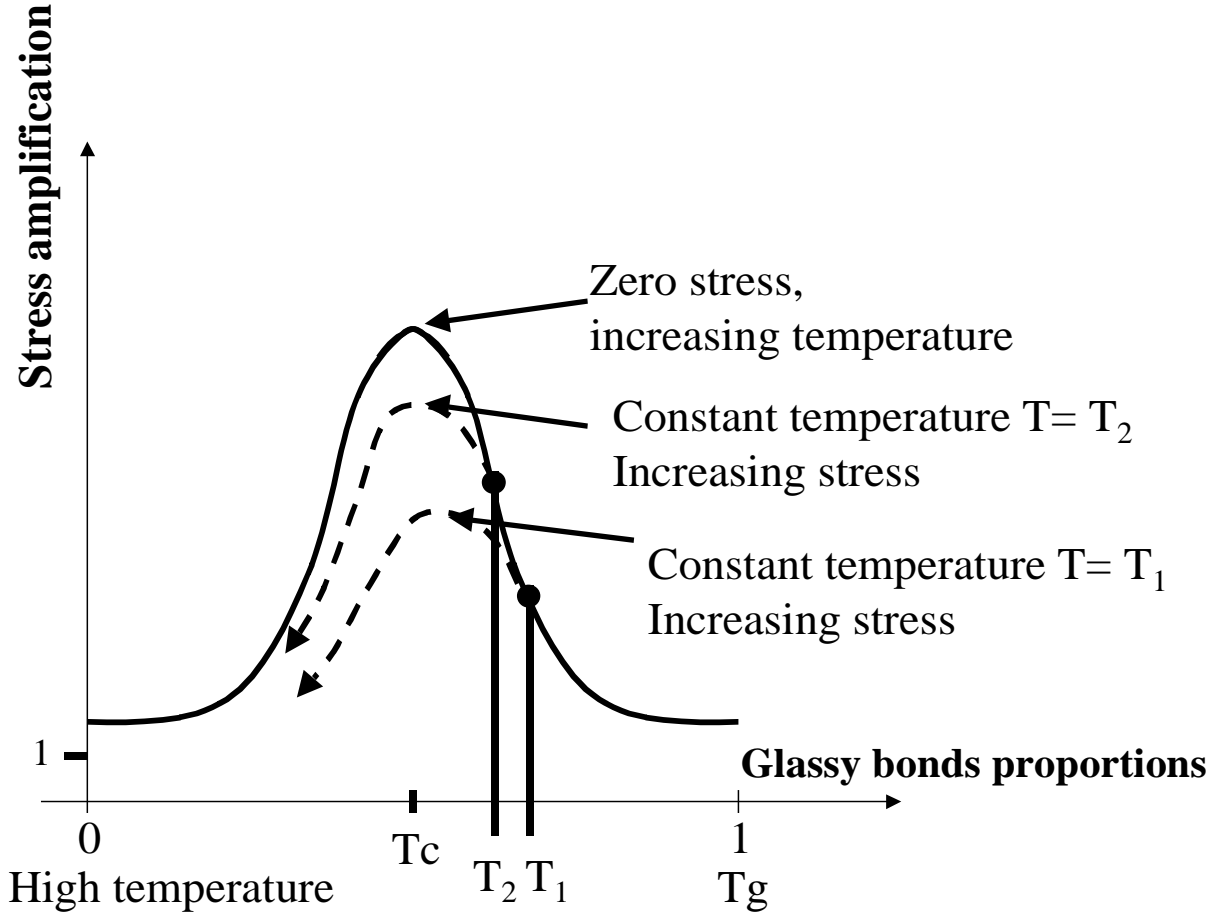


Figure 8: Schematic representation of the stress amplification factor versus the fraction of glassy bonds. While increasing temperature the glassy bonds are molten progressively, moving from right to left (solid line). The bond network goes through a percolation threshold at  $T_c$ . At this temperature, the stress localisation and so the stress amplification are maximal. An increase of strain amplitude leads to a similar decrease of glassy bonds numbers. A bell like shape for the amplification factor is obtained again (dashed line). However, in this case the amplification factor increases slower than for a temperature increase. The maximum of the amplification factor observed for increasing strain is then temperature dependent. It decreases as temperature increases (see the two dashed lines starting from temperatures  $T_1$  and  $T_2$  and figure 6b)

## Conclusion

We have analyzed in this work the origin of the precocious non-linear viscoelastic behavior observed on model filled elastomers composed by cross-linked polyethylacrylate chains reinforced with grafted silica nanoparticles. Our approach is based on the existence of a glass transition gradient near the particle surfaces. This approach, as shown in ref [13], accounts for the temperature and frequency variations of the linear viscoelastic modulus of filled elastomers. We show in this work that the precocious non-linear viscoelastic behavior observed for increasing macroscopic deformation on these filled elastomers can be attributed to the strain-softening of a part of the glassy polymer that we have assumed to be similar to strain-softening in bulk at the corresponding  $T_g$ . In this frame, we can predict a temperature–frequency superposition law for the non-linear elastic modulus that is validated by experiments. Moreover, we can compare the effect of temperature with the effect of strain amplitude on the softening of the glassy shells. It appears that the stress effect is quite complex. First there is an important amplification factor between the macroscopic stress and the local stress. This is consistent with the fact that more disordered the sample is, the larger is the shift between stress and temperature dynamical modulus. Secondly, the shift factor between stress and temperature dynamical modulus exhibits a pronounced maximum which may correspond to the percolation threshold of the skeleton constituted by glassy bridges connecting neighboring particles. This is consistent the variation of the mechanical behavior with temperature observed for our samples. When there is no stress amplification – i.e. in very well dispersed samples- , the strain-softening should occurred at very high macroscopic strain ( $> >100\%$ ) and should be weak. Lastly, all this picture explains the slow recovery of the samples after either a temperature quench (above  $T_g$ ) or the cessation of a mechanical loading. It is also in agreement with the fact the response becomes “apparently linear” after a few cycles. These last effects are in fact reminiscent from the properties of glassy polymers.

Finally, the effect of particles arrangements - on the precocious strain-softening, or Payne effect, in reinforced elastomers - remains still puzzling. We were able to show that the stress-softening of the glassy shells surrounding the solid particles is responsible for this effect. But we have also observed that its amplitude is very dependent on the arrangement of the particles through both the local stress amplification but also through the dependence of the local stress redistribution on the stress amplitude. Thus we expect that new approaches taking precisely into account the particles arrangement under stress (like in [3]), but including our effect of strain-softening of glassy chains, would be very efficient to describe the complex properties of filled elastomers.

## Acknowledgement :

We thank C. Fretigny for very helpful discussions.

## References :

- (1) Kraus G. *J. Appl. Polym. Sci-Appl. Polym. Symp.* **1984**,39,75
- (2) Witten T.A., Rubinstein M. and Colby R. H., *J. Phys. II*, **1993**, 3, 367
- (3) Huber G. and Vilgis T. A. *Macromolecules* **2002**, 35, 9204
- (4) Heinrich G., Klüppel M. and Vilgis T.A., *Current opinion in Solid State and Materials Science*, **2002**, 6 195, Heinrich M. and Klüppel G.,
- (5) Maier P.G. Görizt D., *Kautschuk Gummi Kunststoffe* 1996; 49(1):18
- (6) Sternstein S.S. and Zhu A. J. *Macromolecules* **2002**, 35,7262
- (7) Struik, L.C.E., : *Physical Aging in Amorphous Polymers and other Materials* Elsevier, Amsterdam 1978.
- (8) Struik, L.C.E., *Polymer* ,**1987**, 28, 1521.
- (9) Haidar B., Vidal A. Papirer E., *Proceeding, Eurofillers 97*, Manchester (UK) September 8th – 11th, **1997**, 239.; Haidar B, Salah Deradji H. Vidal A., Papirer E., *Macromol. Symp.* **1996**, 108, 147.
- (10) Kaufmann S, Slichter WP, Davis DD, *Jour. Polymer. Sci. A2*, **1971**, 9, 829.
- (11) Wang MJ, *Rubber Chemistry and Technology* 1998 ,71, 520

- (12) Berriot J, Lequeux F., Monnerie L., Montes H., Long D., Sotta P., J. Non Cryst. Solids 2002, 310, 719
- (13) Berriot J., Montes H., Lequeux F., Long D. Sotta P., Macromolecules 2002, 35, 9756
- (14) Keddie, J.L., Jones R.A.L. and Cory R.A. Europhys. Lett. 1994, 27, 59-64.
- (15) Forrest, J.L., Dalnoki-Veress, K and Dutcher J.R. Phys. Rev. E. 1997, 56, 5705.
- (16) Fukao K., Miyamoto Y. Phys. Rev. E 2000, 61, 1743
- (17) Grohens, Y., Brogly, M., Labbe, C., David, M.O. and Schulzt, J. Langmuir 1998, 14, 2929
- (18) Starr F.W., Schröder T. B., Glotzer S. C., Macromolecules 2002, 35, 4481
- (19) Starr F.W., Schröder T. B., Glotzer S. C., Phys. Rev. E 2002, 64, 021802
- (20) Long, D. and Lequeux, F. EPJ E. 2001, 4, 371.
- (21) Payne A.R. : Reinforcement of elastomers Chapter 3, G. Krauss ed. , Wiley Interscience, New York 1965
- (22) Berriot J., Montes H., Monnerie L., Martin F., Pyckhout-Hintzen W., Meier G., Frielinghaus H. Polymer, 2002 (submitted).
- (23) Jethmalani, J.M. and Ford, W.T., Chem. Mater. 1996, 8, 2138.
- (24) Mauger M. Thesis University Paris VI
- (25) Berriot J., Martin F., Montes H., Monnerie L Sotta P., Polymer. 2003 2003, 44, 1437
- (26) Berriot, J.; Montes, H.; Lequeux, F.; Pernot, H. Polymer. 2002, 43 ,6131.
- (27) Ward I.M., Mechanical properties of solid polymers, 2nd edition, John Wiley & SONS, 1983
- (28) Ouali N., Mangion M; Perez J., Phil. Mag. 1993, A67, 827
- (29) Brule B., Halary J. L., Monnerie L., Polymer 2001, 42, 9073
- (30) Zhou Z., Chudnovsky A., Bosnyak C.P., Sehanobish K. Polym. Eng. Sci. 1995, 35, 304
- (31) Oleinik E.F., Shenogin S.V., Paramzina T.V, Rudnev S.N., Shantarovich V.P., Azamatova Z.K., Pakula T., Fischer E.W. Polym. Sci. Serie A, 1998, 40, 1187.
- (32) Rabinowitz S., Beardmore P., J. Mater. Sci. 1974, 9, 81
- (33) Isayev A. I., Katz D., Intern. J. Polymeric Mater. 1980, 8, 25
- (34) Chazeau L., Brown J.D., Yanyo L.C. Sternstein S.S Polym. Compos. 2000, 21, 202
- (35) Lapra A. Thesis University of Paris VI 1999
- (36) For the strain field around a solid inclusion see for instance in Palierne J.F. Rheologica Acta 1990 29, 204